IEEE Access
Multidisciplinary | Rapid Review | Open Access Journal

IEEE ENGINEERING IN MEDICINE AND BIOLOGY SOCIETY SECTION

Received 14 April 2024, accepted 13 May 2024, date of publication 16 May 2024, date of current version 3 June 2024.

Digital Object Identifier 10.1109/ACCESS.2024.3402075

RESEARCH ARTICLE

An EEG-Based Seizure Recognition Method Using Dynamic Routing

ZHIWEN XIONG[1], YANG LIU[2], AND PENG JIANG[1]
[1]Yiwu Industrial and Commercial College, Jinhua 322000, China
[2]Chongqing College of Science and Creation, Chongqing 402160, China

Corresponding author: Peng Jiang (ywiccjp@ywicc.edu.cn)

This work was supported by Fund Projects: Zhejiang Province Philosophy and Social Science Planning Project under Grant 20NDJC344YBM.

ABSTRACT The diagnosis and treatment of brain diseases represent the forefront of brain science research, with EEG-related research occupying a uniquely significant position. In recent years, deep learning technology has been widely applied to the study of EEG signals, yet the integration of information from multiple EEG channels remains a challenging task. Based on the dynamic routing algorithm, this study established a deep neural network. Subsequently, leveraging this network, an epileptic seizure recognition method, VarChanNet, was proposed. Seizure recognition experiments were conducted using the Bonn and CHB-MIT databases. The experimental results demonstrate that the proposed VarChanNet method maintains high recognition accuracy even when the number of channels involved in the recognition process changes. It reliably functions on both the Bonn and CHB-MIT databases, indicating its potential for generalization. Furthermore, the method provides recommendations for channel selection during the recognition process. For instance, in the case of CHB-MIT, Channel 21 can be selected for single-channel recognition, Channels 2 and 3 for dual-channel, and Channels 1, 2, and 3 for triple-channel epileptic seizure recognition. In a word, the proposed VarChanNet method enables the fusion of information from different EEG channels, supporting recognition tasks even when the number of channels varies. It offers a new perspective for EEG analysis and holds the potential for generalization.

INDEX TERMS Electroencephalography, capsule neural network, dynamic routing algorithm, brain connectivity, seizure detection.

I. INTRODUCTION

In order to accurately diagnose whether a patient is suffering from epilepsy, it is imperative to recognize epileptic seizures through the meticulous analysis of EEG signals. The objective of epileptic EEG signal recognition lies in precisely identifying epileptic seizure states by thoroughly examining these signals. Epileptic seizures are brain disorders that result from excessive firing of brain neurons, and this aberrant neuronal discharge is referred to as epileptic discharge. This epileptic discharge manifests as ''abnormal waves'' within EEG signals, primarily encompassing spike waves, sharp waves, spike-slow waves, sharp-slow waves, and other similar patterns. Essentially, epileptic EEG signal recognition involves the detection of these ''abnormal waves''. Therefore, to accurately assess whether a patient has epilepsy, it is crucial to observe their clinical manifestations and perform epileptic seizure recognition [1] based on the analysis of EEG signals.

The primary techniques for extracting features from EEG signals encompass time domain analysis [2], frequency domain analysis [3], time-frequency domain analysis, and nonlinear dynamics methods. These techniques involve extracting features from the EEG signals in the time domain [4], frequency domain, time-frequency domain [5], or nonlinear dynamics [6]. Subsequently, classical classifiers are employed to categorize these extracted features, enabling recognition. The approach involves a combination of ''feature extraction'' and ''classical classifier''. Initially,

The associate editor coordinating the review of this manuscript and approving it for publication was Carmen C. Y. Poon.

features are extracted from EEG signals across various domains, including time, frequency, time-frequency, and nonlinear dynamics. These features are then characterized and used as input data for classical classifiers to facilitate recognition. Commonly used classical classifiers include linear discriminant analysis [7], decision tree [8], support vector machine [9], K-nearest neighbor [10], and Naive Bayes [11], [12].

In recent years, deep neural networks [13] have yielded promising results in the analysis of time series signals, such as in signal detection tasks [14]. Consequently, some studies have leveraged deep neural networks [15] to analyze EEG signals and detect epileptic seizures. Raw data from EEG segments or manually extracted features can serve as input data for these deep neural networks. However, it's worth noting that the dimensionality of the input data impacts the dimensionality of the convolutional units employed by the deep neural network. Typically, since the input data has a relatively low dimension, the convolutional units also tend to have a lower dimension. Currently, when deep neural networks are utilized to recognize epileptic EEG signals, the convolutional units are often one-dimensional (1D) [16], [17], two-dimensional (2D) [18], [19], or even three-dimensional (3D).

Various deep neural networks, such as convolutional neural networks (CNN) [20], recurrent neural networks (RNN) [21], [22], autoencoders (AE), deep belief networks (DBN) [23], and innovative hybrids jointly constructed by multiple neural networks, have been extensively employed in the field of seizure recognition research.

The number of EEG channels used in different studies of seizure recognition varies. Some studies use only data from a single channel, which requires less computation but also obtains less effective information from EEG signals. At the same time, there are also studies that use data from all EEG channels, which requires more computation but also obtains more information from EEG signals. In addition, some studies select a subset of all EEG channels for epilepsy seizure recognition, which requires selecting the most appropriate channel subset. Currently, most studies use fixed EEG channels, and information can only be extracted from pre-selected channels and fused to achieve recognition. In order to better find the appropriate channel combination, when the number of involved channels needs to be changed, most existing studies are unable to cope with it. Therefore, in order to ensure that the EEG recognition method can still operate effectively when the number of channels involved in the recognition operation changes, it is crucial to solve the problem of fusing variable-sized channel data.

In the context of epilepsy seizure detection based on deep learning technology, it is important to effectively cope with changes in the number of channels. This is the motivation of this paper. In order to effectively extract recognition information from the data of each channel when the number of channels changes, this paper proposes a deep neural network-based VarChanNet method. In addition, this study uses the Bonn database and CHB-MIT database for experiments, and based on the experimental results, the performance of VarChanNet method under different channel numbers is analyzed. VarChanNet provides a new research direction for epilepsy seizure detection in scenarios with varying channel numbers.

II. METHOD DESCRIPTION

In this paper, a thorough exposition is presented of VarChanNet, a cutting-edge recognition method for seizures. This comprehensive description encompasses the dynamic routing algorithm, the intricate structure of the deep neural network that relies on this algorithm, and the loss function. Within the framework of VarChanNet, a method for seizure recognition through EEG signals is established, grounded in the innovative 1D-capsule approach that is built upon the dynamic routing algorithm. The intricate network structure is clearly depicted in Figure 1, revealing its sophisticated composition of five layers.

The first layer is to extract the EEG channel data involved in the recognition operation from the EEG segment named Segment i ($1 \leq i \leq n$) as the input data of the 1D-Capsule, where n is the total number of EEG segments. In Figure 1, the 1D-capsule has three channels participating in the recognition operation: Channel A ($1 \leq A \leq m$), Channel B ($1 \leq B \leq m$) and Channel C ($1 \leq C \leq m$) as the channels participating in the recognition operation, where m is the total number of channels contained in the EEG segment. The data of the three channels involved in the recognition operation at the first layer were convolved and ReLU was performed to obtain the characteristic matrix of the second layer. Convolved the feature matrix of the second layer again to obtain the feature matrix of the third layer, that is, the feature matrix in the PrimaryCaps layer;. The feature matrix in the PrimaryCaps layer is encapsulated into capsules containing 16 values(16D), and the fourth layer is obtained, that is, 1952 in the capsules layer × Three 16D capsules, of which 1952 capsules are obtained from the input data of each EEG channel after calculation; The fifth layer is DigitCaps layer, capsules in Capsules layer are used as the input of dynamic routing algorithm, and two capsules are obtained after operation. The vector lengths of the two capsules correspond to the prediction probability of Seizure or Non-Seizure type of current EEG segment respectively. The class with the highest probability is the recognition result of the current EEG segment, and the operation process of each layer in the 1D-Capsule is as follows:

(1) In the first layer, each EEG channel contains 256 values, and the convolution operation for each channel is set as $kernel_{size}$ =9,$stride$ = 1,$out_{channels}$ = 64. ReLU operation is performed after Convolution. Each channel can obtain data of 64 × 248 dimensions in ReLU layer of Convolution.

(2) In the second layer, the corresponding data dimension of each channel is 64 × 248 , and the convolution operation is set as $kernel_{size}$ = 5, $stride$ = 2, $out_{channels}$ = 256.

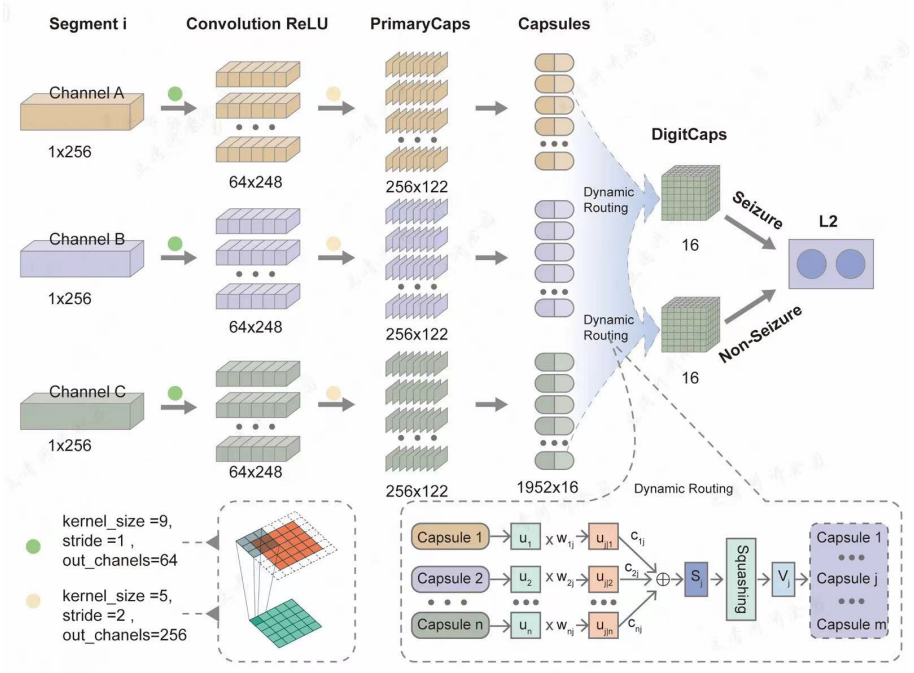

FIGURE 1. The network structure of 1D-capsule.

After completing the convolution, each channel can obtain 256×122 data in the PrimaryCaps layer.

(3) In the third layer, the data dimension corresponding to each channel is 256×122 , which is first converted into one-dimensional data with a dimension of 1×31232 , and then again into data with a dimension of 1952×16 , and a total of 1,952 16-bit (16D) data are obtained, which is called 1,952 16D capsules. In Figure 1, as the data of three channels were used as input of the 1D-capsule, a total of $1,952\times3 = 5,856$ 16D capsules were obtained.

(4) The fourth layer contains 5856 16D capsules, these capsules can be obtained through the dynamic routing algorithm, 2 16D capsules in DigitCaps layer, the specific implementation details are as follows:

The capsules of DigitCaps layer in 1D-capsule are obtained by the capsules in Capsules layer through dynamic routing algorithm. Dynamic routing algorithm specific calculation process such as Algorithm 1. As shown, each capsule in the Capsules layer corresponds to a vector u_i, and the vector v_j corresponding to each capsule in the DigitCaps layer is obtained through the dynamic routing algorithm.

The dynamic routing algorithm used to generate the capsules in DigitCaps layer with capsules in Capsules layer is described as follows:

Algorithm 1 describes how to generate high-level capsules from low-level capsules. Firstly, u_i $(i = 1, 2, \ldots, n)$ multiply by weight matrix W_{ij} (j is the number of capsules in DigitCaps layer), as shown in Formula 1:

$$\hat{u}_{j|i} = W_{ij}u_i \tag{1}$$

Among them, $W_{ij}$is the transformation matrix between u_i and $\hat{u}_{j|i}$ with a dimension of 16×16, which is used to describe the relative spatial relationship between low-level features and high-level features, which is maintained by 1D-Capsule during training renew.

Then, line 7 to 10 is iterated T times to obtain v_j. Which $\hat{u}_{j|i}$ sum after multiplied by their weights, the result is stored in the s_j. The calculation method is shown in Formula 2:

$$s_j = \sum_i c_{ij}\hat{u}_{j|i} \tag{2}$$

where c_{ij} is the coupling coefficient of u_i and the jth (jth) capsule in DigitCaps layer, and c_{ij} satisfies the conditions shown in Formula 3:

$$\sum_i c_{ij} = 1 \tag{3}$$

The calculation method of c_{ij} is shown in Formula 4:

$$c_{ij} = \frac{exp\left(b_{ij}\right)}{\sum_k exp\left(b_{ik}\right)} \tag{4}$$

Among them, the initial logit (initial logit) b_{ij} is the log prior probability (Log prior probability) of the combination of u_i and the jth capsule in DigitCaps layer.

In Algorithm 1, the nonlinear function named squash is used to compress s_j to ensure that the vector length of v_j corresponding to jth capsule is between 0 and 1. Its calculation method is shown in Formula 5:

$$v_j = \frac{||s_j||^2}{1 + ||s_j||^2}\frac{s_j}{||s_j||} \tag{5}$$

Algorithm 1 Dynamic Routing Algorithm

Require: The vector u_i corresponding to the capsule in the Capsules layer, the number of iterations is T

Ensure: Capsule v_j in DigitCaps layer

for $j = 1; j \leq m; j++$ **do**
  for $i = 1; i \leq n; i++$ **do**
    $b_{ij} = 0$ //Initialize variables
    $\hat{u}_{j|i} = W_{ij} u_i$
  end for
  for $r = 1; r \leq T; r++$ **do**
    $c_{ij} = softmax(b_{ij})$
    $s_j = \sum_i c_{ij} \hat{u}(j|i)$
    $v_j = squash(s_j)$
    $b_{ij} = b_{ij} + \hat{u}_{j|i} \times v_j$
  end for
  return v_i
end for

The 1D-capsule automatically changes the network structure based on the number of channels involved in the recognition operation. Although the change of the number of channels would lead to the change of the number of capsules in the Capsules layer, the dynamic routing algorithm could still calculate the capsules in the DigitCaps layer.

The loss function designed in 1D-Capsule is shown in Formula 6:

$$Loss = L_1 + L_2 \tag{6}$$

Loss is the total loss function, L_1 is the loss when the 1D-Capsule predicts the EEG segment as a Seizure class, and L_2 is the loss when the 1D-Capsule predicts the EEG segment as a Non-Seizure class. The calculation method of L_k is shown in Formula 7:

$$\begin{aligned} L_k = \ & T_k max(0,\ 0.9 - ||v_k||)^2 \\ & + \lambda \left(1 - T_k\ max\ (0,\ ||v_k|| - 0.1)^2\right) \end{aligned} \tag{7}$$

where max is the largest set element, and its calculation method is shown in formula 8.

$$\begin{cases} max(x, y) = x, x \geq y \\ max(x, y) = y, x < y \end{cases} \tag{8}$$

k in Formula 7 is the number of categories in the Digitcaps layer. There are two values of K. when $k = 1$, L_k represents the loss when the EEG segment is predicted to be seizure class. When $k = 2$, L_k represents the loss when the EEG segment is predicted to be non seizure.

Algorithm 2 Pseudocode of VarChanNet

Require: EEG data EEG_{data}, "Sliding time window length" $window_{len}$, number of channels involved in the recognition operation $chan_{number}$

Ensure: $identification_{results}$ of all EEG fragments in the test set

// Get all EEG segments
$data = EEG_{split}(EEG_{data}, window_{len})$
// Split into training and test set
$sample_{train},\ sample_{test}, = split(data)$
// Building a deep neural network
$network = net(chan_{number})$
// If using existing weights
if Trained weights is used **then**
  // Load trained weights
  $load_{weights}(network,\ The\ trained\ weights)$
end if
// Train the network
$train_{network}(network,\ sample_{train})$
// Identify with the network
$identification_{results} = test_{network}(network, sample_{test})$
return

When training 1D-Capsule with EEG segments, when the category of EEG segment is accurately predicted to be $i (i \leq k)$: $T_i" = 1"$, if the category of EEG segment is predicted to be i and the prediction result is wrong: $T_i" = 0"$.

λ in Formula 7 represents the specific gravity of FP and FN on L_k. $\lambda = 0.5$ is set, that is, FP increases the loss function twice as fast as FN. $||v_k||$ is a vector length, including v_k is calculated by using dynamic routing algorithm, also corresponds to the capsule of the first category k vector.

(5) The fifth layer consists of two 16D capsules. The vector lengths of the two capsules correspond to the predicted probability of Seizure or Non-Seizure of the current EEG segment, and the category with the highest probability is the result of the recognition of the current EEG segment.

When VarChanNet method is used for recognition of epileptic seizures, the internal data stream is shown in Figure 2, which needs to be processed by four modules, which are acquisition of original EEG data, preprocessing, segmentation, and recognition.

The process of VarChanNet method for recognition is shown in Algorithm 2. Firstly, EEG segments were

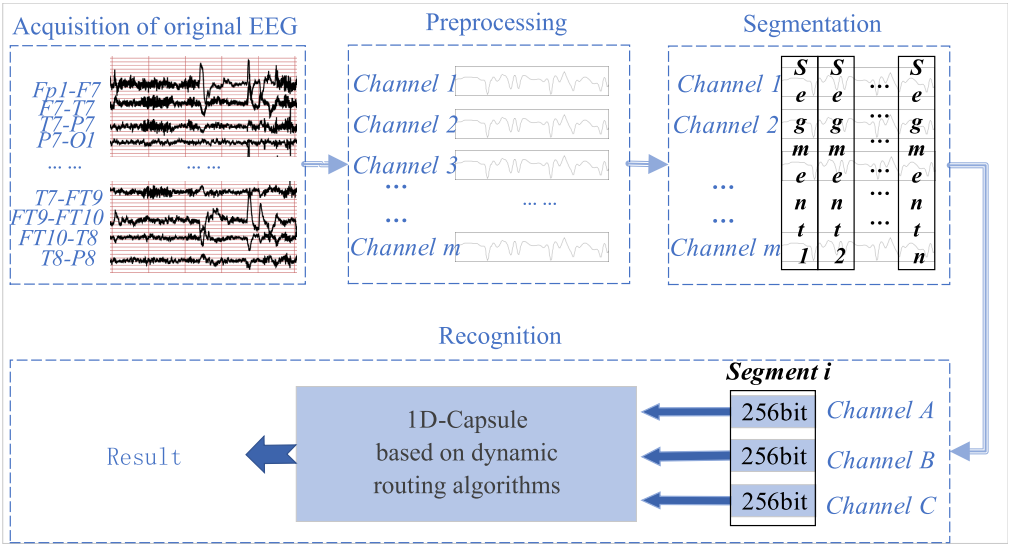

FIGURE 2. The data flow of EEG recognition using VarChanNet.

segmented from EEG data by sliding time window, and the EEG segments were divided into training set and test set as the input data of the 1D-Capsule. Secondly, the network structure of the 1D-Capsule was determined according to the number of channels participating in the recognition operation. Finally, the network trained can be used to recognize seizures.

III. EXPERIMENTAL SCHEME

This section introduces performance evaluation metrics, describes the publicly available epileptic EEG database used in the experiment, and clarifies the experimental design.

A. EXPERIMENTAL DATABASE AND PERFORMANCE EVALUATION INDEX

1) DATABASE

In the experiment, the Bonn database and the CHB-MIT database were employed, both of which are frequently utilized public EEG databases in epileptic research. Notably, the Bonn database comprises single-channel EEG recordings, whereas the CHB-MIT database features multi-channel EEG data. All EEG recordings in the CHB-MIT database were gathered using the internationally standardized 10-20 electrode placement system, with lead information detailed in Table 1.

It should be pointed out that FT9 and FT10 channels do not belong to the 10-20 international system. In order to explain the problem, we use the 10-10 system when necessary. Besides, due to the naming modification of the 10-20 international standard system, the middle temporal electrode markers changes from T3/T4 to T7/T8, T5/T6 to P7/P8. Synthesizing information of CHB-MIT database, the electrode positions of CHB-MIT database (Figure 3-a) and Channel 23 (Figure 3-b) are obtained. The midpoint of each channel is taken as the channel position marker, as shown is Figure 3-c (According to the table, it can be seen that electrodes of Channel 3 and Channel 9 are the same but directions are different, and electrodes of Channel 15 and Channel 23 are the same but directions are different).

2) EVALUATION INDEX

In order to evaluate VarChanNet, Accuracy is taken as the evaluation index. The calculation method is as follows:

$$Accuracy = \frac{(TP + TN)}{(TP + FP + TN + FN)} \tag{9}$$

TP: The prediction of a certain EEG segment belonging to the status of epileptic seizure and the prediction is correct; FP: The prediction of a certain EEG segment belonging to the status of epileptic seizure, but the prediction is incorrect; TN: The prediction of a certain EEG segment not belonging to the status of epileptic seizure and the prediction is correct; FN: The prediction of a certain EEG segment not belonging to the status of epileptic seizure, but the prediction is incorrect.

3) INSPECTION OF RESULTS

Based on EEG experiments, when changing the number of channels, we can obtain a large amount of data from single-channel, dual-channel, and triple-channel combinations. For 23-channel EEG, there are 253 combinations of two channels and 1771 combinations of three channels. In order to more clearly illustrate the algorithm, this section uses single-channel data for experiments, selecting data from channels 1 to 23. When using dual-channel and triple-channel experiments, we select channels 1 to 5 and obtain 10 sets of dual-channel combinations and 10 sets of triple-channel combinations. In most cases in nature, when the amount of data is large enough, these data tend to be approximately normal distributed. Therefore, although the experiment selects some combinations for testing, their results are representative.

TABLE 1. Lead information table.

Channel number	Corresponding electrode	Channel number	Corresponding electrode	Channel number	Corresponding electrode
1	FP1-F7	9	FP2-F4	17	FZ-CZ
2	F7-T7	10	F4-C4	18	CZ-PZ
3	**T7-P7**	11	C4-P4	19	**P7-T7**
4	P7-O1	12	P4-O2	20	T7-FT9
5	FP1-F3	13	FP2-F8	21	FT9-FT10
6	F3-C3	14	F8-T8	22	FT10-T8
7	C3-P3	15	**T8-P8-0**	23	**T8-P8-1**
8	P3-O1	16	P8-O2		

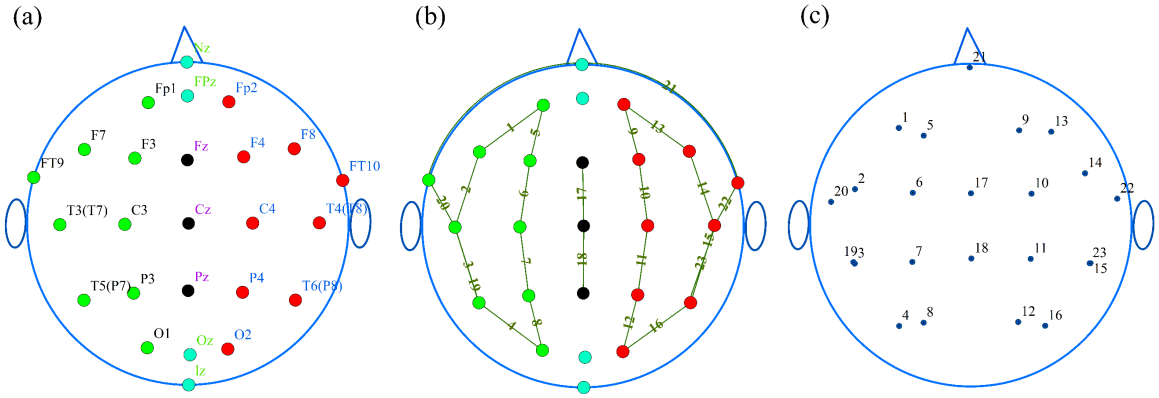

FIGURE 3. CHB-MIT database electrode and channel schematic.

Therefore, in this study, a normality test was conducted on the experimental results. If the recognition accuracy follows a normal distribution, then they are representative. If it does not follow a normal distribution, then additional data needs to be added for further analysis.

B. EXPERIMENTAL DESIGN

The experiment was conducted based on the Bonn database and the CHB-MIT database, with the following details:

(1) Experiment 1: Conducting experiments on the Bonn database.

The first experiment was conducted on the Bonn database, with a channel number of 1 for VarChanNet recognition operation. All EEG segments generated from Set D and Set E were mixed together, with 80% randomly assigned to the training set and 20% assigned to the test set. The experiment was tested using a dichotomy method to determine whether each EEG segment was during a seizure or not. The 1D-Capsule training was performed for 50 rounds, and the evaluation metric values were obtained using the test set after each round of training. The evaluation metric statistics were divided into two parts: the first part calculated the average value of the metrics for the last 10 rounds of network training, which was the Accuracy Ave; the second part calculated the maximum value of the metrics during the 50 rounds of training, which was the Accuracy Best.

TABLE 2. The results of experiment 1.

Evaluation index	Ave	Best
Accuracy	0.972031	0.975

Experiment 1 objective: On the Bonn database, when the number of channels involved in recognition operations is 1, perform seizure recognition.

(2) Experiment 2: Conducting experiments on the CHB-MIT database.

Experiment 2 was conducted on the CHB-MIT database, with the number of channels participating in the recognition operation being 1, 2, and 3. When the number of channels was 2, there were two experimental schemes: one was to select two channels from channel 1 to channel 5 for experimentation, and the other was to select the two channels with the highest Accuracy Ave from channel 1 to channel 5 based on the single-channel test results. Similarly, when the number of channels was 3, there were also two experimental schemes. The data of each participant was divided into training data and test data. In order to more concisely present the experimental results, the experiments of participants chb01 and chb10 were taken as examples for explanation.

TABLE 3. Experiment results for single-channel.

Channel	chb01		chb10	
	Avg Accuracy	Best Accuracy	Avg Accuracy	Best Accuracy
1	0.9381	0.9524	0.8977	0.9128
2	0.9232	0.9464	0.9622	0.9826
3	0.9137	0.9286	0.9767	0.9767
4	0.8845	0.8929	0.9541	0.9651
5	0.9351	0.9464	0.7837	0.8081
6	0.9054	0.9286	0.8041	0.8256
7	0.8643	0.8810	0.8994	0.9128
8	0.8786	0.9048	0.9424	0.9477
9	0.9345	0.9405	0.7576	0.7733
10	0.8702	0.8810	0.7890	0.8140
11	0.9101	0.9107	0.8337	0.8488
12	0.8607	0.8690	0.8576	0.8663
13	0.9458	0.9583	0.7012	0.7209
14	0.9298	0.9405	0.8308	0.8430
15	0.9256	0.9286	0.8297	0.8372
16	0.8804	0.8929	0.8837	0.9012
17	0.8268	0.8452	0.7965	0.8081
18	0.8518	0.8690	0.8302	0.8430
19	0.9155	0.9226	0.9767	0.9826
20	0.9030	0.9107	0.9640	0.9651
21	0.9542	0.9583	0.9477	0.9535
22	0.9530	0.9583	0.7994	0.8081
23	0.9268	0.9345	0.8221	0.8372

Experiment 2 objective: To analyze the effects of varying the number of channels and combinations of channels involved in seizure recognition.

IV. EXPERIMENT RESULTS AND ANALYSIS

A. EXPERIMENT RESULTS

(1) Experiment 1: The results of experiments carried out on Bonn database: as shown in Table 2.

(2) Experiment 2: The results of experiments carried out on CHBMIT database.

① Experiment results when the number of channels involved in recognition operation is 1(single-channel)

As shown in Table 3, the experiment results show the recognition results of VarChanNet based on chb01 and chb10 in single-channel mode.

② Experiment results when the number of channels involved in recognition operation is 2(two-channel)

As shown in Table 4, the experiment results show the recognition results of VarChanNet based on chb01 and chb10 in two-channel mode.

③ Experiment results when the number of channels involved in recognition operation is 3(three-channel)

As shown in Table 5, the experiment results show the EEG signal recognition results of VarChanNet based on chb01 and chb10 in three-channel mode.

B. RESULT ANALYSIS

(1) Analysis of experiment results when the number of channels involved in recognition operation is 1(single-channel).

The recognition results are statistically analyzed and Shaprio-Wilk is used to test the normal distribution. The results are shown in Table 6 and Figure 4. It can be seen that Acc indexes obtained from chb01 and chb10 obey normal distribution, and the data obtained are reliable. The statistical average of the recognition results of chb01 and chb10 shows that the result of chb01 is better than that of chb10. Rank the experiment results of chb01 single-channel in order of Accuracy Ave for top 5, and it can be obtained that Channel 21>Channel 22>Channel 13>Channel 1>Channel 5. Rank the experiment results of chb10 single-channel in order of Accuracy Ave for top 5, and it can be obtained that Channel 3>Channel 19>Channel 20>Channel 1>Channel 4. It is indicated that the change of channels can affect the accuracy of the recognition results and the optimal single channel is different for different patient samples.

Take the midpoint of Channel 23 as the channel coordinate (the electrodes of Channel 3 and Channel 9 are the same but directions are different, and average to assign the midpoint coordinate; the electrodes of Channel 15 and Channel 23 are the same but directions are different, and average to assign the midpoint coordinate), assign the channel coordinate

TABLE 4. Experiment results of two-channel.

Channel	chb01		chb10	
	Accuracy Ave	Accuracy Best	Accuracy Ave	Accuracy Best
1,2	0.958333	0.958333	0.9465	0.988372
1,3	0.942262	0.946429	0.97615	0.982558
1,4	0.940476	0.946429	0.916861	0.947674
1,5	0.951786	0.958333	0.887791	0.918605
2,3	0.956548	0.958333	0.978488	0.994186
2,4	0.939286	0.946429	0.961628	0.982558
2,5	0.943452	0.952381	0.937791	0.959302
3,4	0.923214	0.928571	0.96686	0.982558
3,5	0.932738	0.946429	0.968605	0.97093
4,5	0.927976	0.940476	0.848256	0.94186

TABLE 5. Experiment results of three-channel.

Channel	chb01		chb10	
	Accuracy Ave	Accuracy Best	Accuracy Ave	Accuracy Best
1,2,3	0.958333	0.964286	0.965116	0.97093
1,2,4	0.938691	0.958333	0.944186	0.965116
1,2,5	0.955952	0.964286	0.936628	0.947674
1,3,4	0.950595	0.958333	0.95	0.97093
1,3,5	0.950595	0.964286	0.97093	0.982558
1,4,5	0.954762	0.964286	0.955233	0.97093
2,3,4	0.947619	0.952381	0.95407	0.959302
2,3,5	0.94881	0.952381	0.924419	0.965116
2,4,5	0.93631	0.946429	0.950581	0.976744
3,4,5	0.95	0.964286	0.959302	0.976744

TABLE 6. Single-Channel and intra-patient mode normal distribution test of experiment results for chb01 and chb10.

Data Number	chb01		chb10	
Evaluation Index	**Acc Ave**	**Acc Best**	**Acc Ave**	**Acc Best**
Analysis Number	23	23	23	23
Average	0.9057	0.9174	0.8626	0.8754
Standard Deviation	0.0349	0.0328	0.0790	0.0751
Average SE	0.0073	0.0068	0.0165	0.0157
Statistics	0.9475	0.9337	0.9360	0.9317
p value	0.2601	0.1314	0.1476	0.1189
Conclusion	+	+	+	+

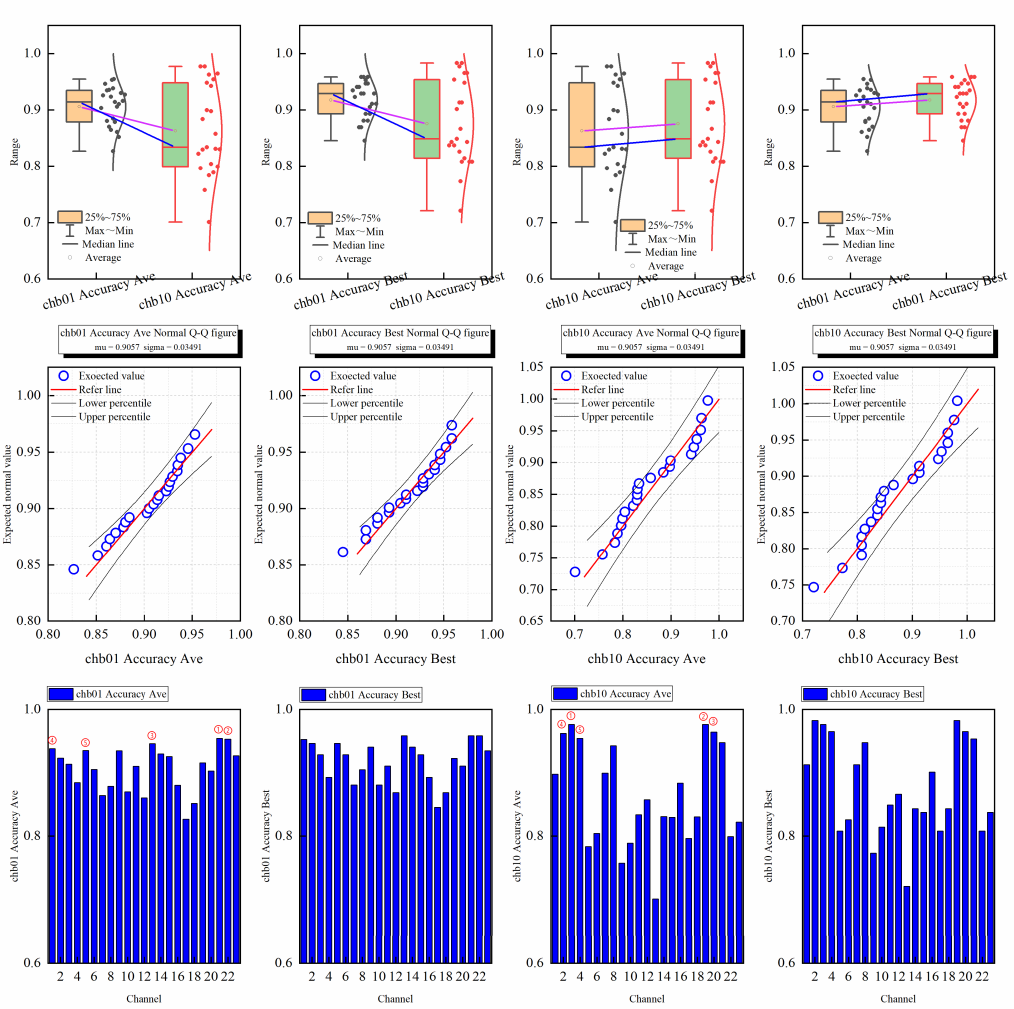

FIGURE 4. Statistical chart of recognition results for single-channel chb01 and chb10.

with the accuracy of Channel 23, and the recognition accuracy distribution of Channel 23 is obtained, as shown in Figure 5. It can be seen that although chb01 and chb10 show different recognition accuracy on different channels, they both show high accuracy on some channels, such as 21,2,3, corresponding to electrodes FT9 and FT10, F7 and T7, T7 and P7. T7 appears twice in high-precision channels, which may suggest that collecting EEG information in certain brain areas for different patients can improve the recognition accuracy of epilepsy.

(2) Analysis of experiment results when the number of channels involved in recognition operation is 2(two-channel).

The recognition results are statistically analyzed and Shaprio-Wilk is used to test the normal distribution. The results are shown in Table 7 and Figure 6. It can be seen that Acc indexes obtained from chb01 and chb10 obey normal distribution, and the data obtained are reliable. The statistical average of the recognition results of chb01 and chb10 shows that, the result of chb01 is better than that of chb10 in terms of Acc Ave index but the result of chb10 is better than that of chb01 in terms of Acc Best index. Rank the experiment results of chb01 two-channel in order of Accuracy Ave, and it can be obtained that Channel 1,2>Channel 2,3>Channel 1,5>Channel 2,5>Channel 1,3>Channel 1,4>Channel 2,4>Channel 3,5>Channel 4,5>Channel 3,4. Rank the experiment results of chb10 two-channel in order of Accuracy Ave, and it can be obtained that Channel 2,3>Channel 1,3>Channel 3,5>Channel 3,4>Channel 2,4>Channel 1,2>Channel 2,5>Channel 1,4>Channel 1,5>Channel 4,5. It is indicated that different combinations of two-channel can affect the accuracy of the recognition results and the optimal two-channel combination is different for different patient samples.

(3) Analysis of experiment results when the number of channels involved in recognition operation is 3(three-channel).

The EEG signal recognition results are statistically analyzed and Shaprio-Wilk is used to test the normal distribution. The results are shown in Table 8 and Figure 7. It can be seen that Acc Best indexes of chb01 disobeys normal

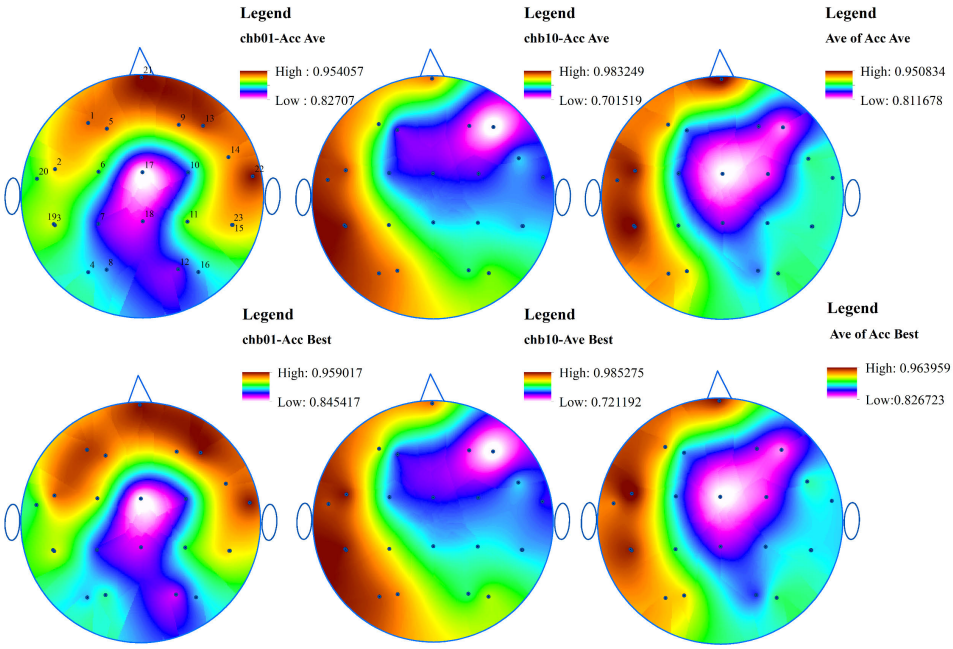

FIGURE 5. Distribution maps of recognition effect of Channel 23.

TABLE 7. Normal distribution test of experiment results for chb01 and chb10 in two-channel and intra-patient mode.

Data number	chb01		chb10	
Evaluation index	Acc Ave	Acc Best	Acc Ave	Acc Best
Analysis number	10	10	10	10
Average	0.94161	0.94821	0.93889	0.96686
Standard deviation	0.01164	0.00933	0.04283	0.02437
Average SE	0.00368	0.00295	0.01354	0.00771
Statistics	0.95959	0.87879	0.85852	0.90286
p value	0.7812	0.12638	0.07331	0.23547
Conclusion	+	+	+	+

+ represents not excluding normality at the 5% level, that is, obeying normal distribution

- represents excluding normality at the 5% level, that is, disobeying normal distribution

distribution, which need more data for further analysis. The analysis of Acc Best indexes of chb01 can only be used as reference. Rank the experiment results of chb01 three-channel in order of Accuracy Ave, and it can be obtained that Channel 1,2,3>Channel 1,2,5>Channel 1,4,5>Channel 1,3,4>Channel 1,3,5>Channel 3,4,5>Channel 2,3,5>Channel 2,3,4>Channel 1,2,4>Channel 2,4,5. Rank the experiment results of chb10 three-channel in order of Accuracy Ave, and it can be obtained that Channel 1,3,5>Channel 1,2,3>Channel 3,4,5>Channel 1,4,5>Channel 2,3,4>Channel 2,4,5>Channel 1,3,4>Channel 1,2,4>Channel 1,2,5>Channel 2,3,5. It is indicated that different combinations of three-channel can affect the accuracy of the recognition results and the optimal three-channel combination is different for different chb samples.

(4) Contrastive analysis of single-channel, two-channel and three-channel.

The averages of Acc Ave and Acc Best of chb01 and chb10 on single-channel, two-channel and three-channel are statistically analyzed. 23, 10 and 10 values of Average of chb01 and chb10 Acc Ave and Average of chb01 and chb10 Acc Best are obtained respectively, as shown in Figure 8.

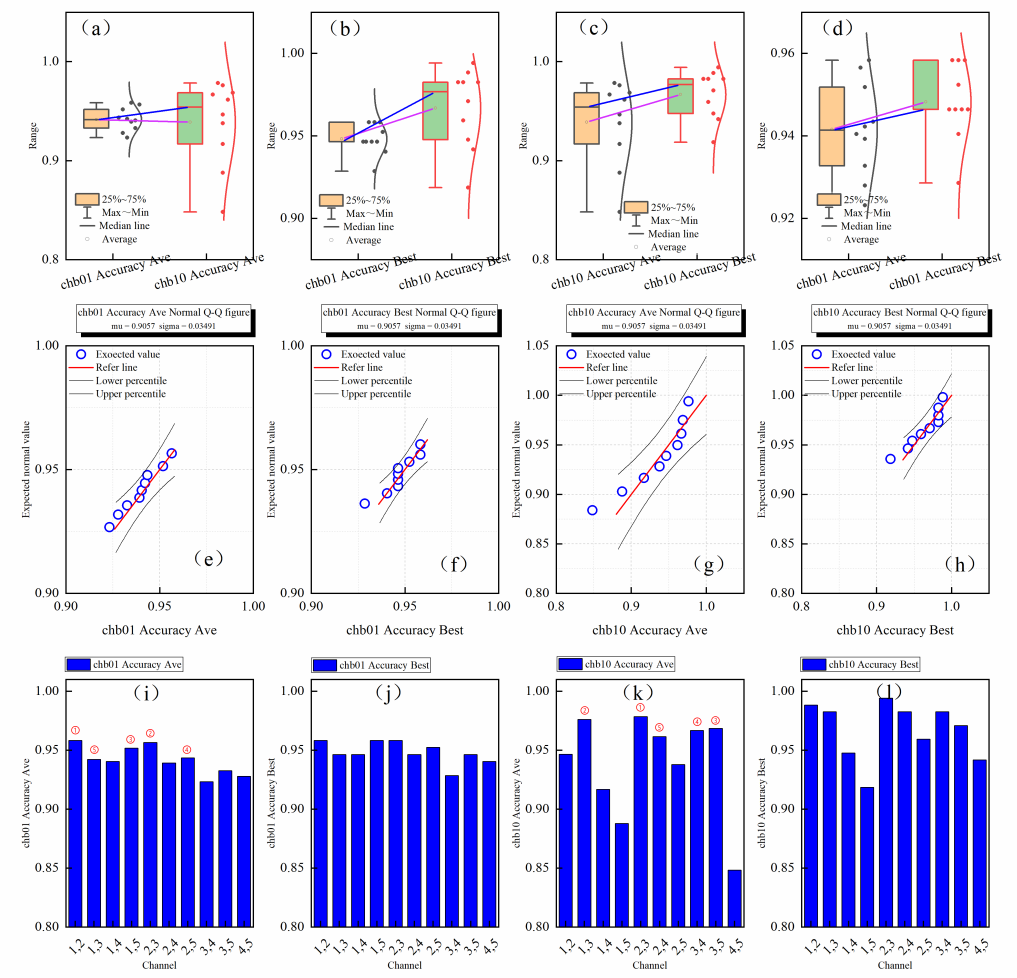

FIGURE 6. Statistical chart of recognition results for two-channel chb01 and chb10.

TABLE 8. Normal distribution test of experiment results for chb01 and chb10 in three-channel and Intra-Patient mode.

Data number	chb01		chb10	
Evaluation index	Acc Ave	Acc Best	Acc Ave	Acc Best
Analysis number	10	10	10	10
Average	0.94917	0.95893	0.95105	0.9686
Standard deviation	0.00702	0.00655	0.01355	0.00996
Average SE	0.00222	0.00207	0.00429	0.00315
Statistics	0.9094	0.80962	0.97148	0.93967
p value	0.27693	0.01897	0.90423	0.54933
Conclusion	+	-	+	+

+ represents not excluding normality at the 5% level, that is, obeying normal distribution

- represents excluding normality at the 5% level, that is, disobeying normal distribution

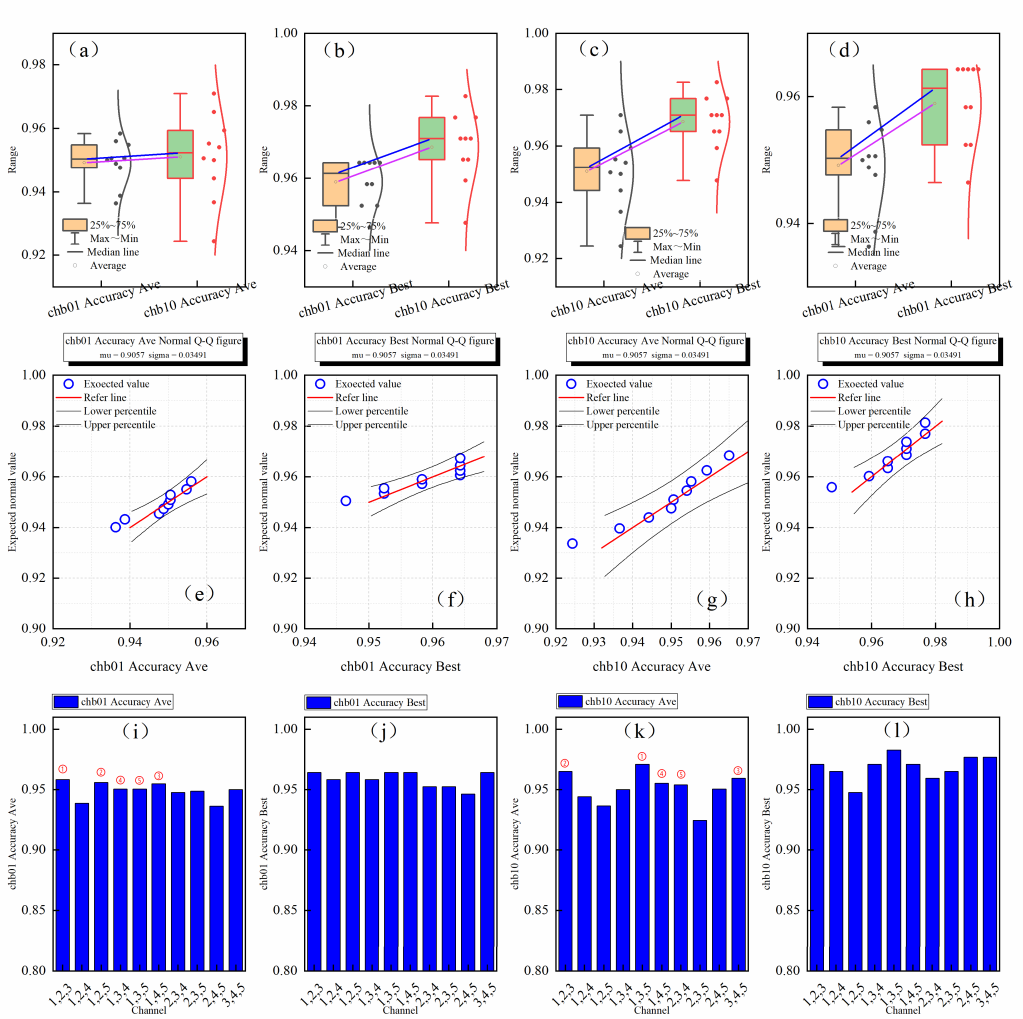

FIGURE 7. Statistical chart of recognition results for three-channel chb01 and chb10.

According to the Accuracy index of chb01 and chb10, chb01 and chb10 both own high Accuracy Ave on Channel 21, and chb01 and chb10 both own high Accuracy Best on Channel 2. Although the maximum recognition accuracy of Channel 2 is optimal on single-channel, the accuracy average is lower than that of Channel 21. If a channel is needed to recognize epileptic EEG signals of chb01 and chb10, relatively high and stable recognition accuracy can be obtained by choosing Channel 21 (Figure 8-a). According to the Accuracy index of chb01 and chb10, chb01 and chb10 own high Accuracy Ave and Accuracy Best when using Channel 2,3, indicating that the combination of Channel 2 and Channel 3 can obtain high and stable recognition accuracy if two channels are needed to recognize epileptic EEG signals of chb01 and chb10 (Figure 8-b). According to the Accuracy index of chb01 and chb10, chb01 and chb10 own high Accuracy Best when using Channel 1, Channel 3 and Channel 5, but the accuracy average is lower than that of Channel 1, Channel 2 and Channel 3. If three channels are needed to recognize epileptic EEG signals of chb01 and chb10, the combination of Channel 1, Channel 2 and Channel 3 can obtain relatively high and stable recognition accuracy (Figure 8-c).

According to the analysis above, the channel combinations with the maximum Acc Ave value of chb01 and chb10 on single-channel, two-channel and three-channel are respectively Channel 21, Channel 2,3 and Channel 1,2,3, the average Acc Ave corresponding to 0.95095,0.967518 and 0.9617245, that is, two-channel>three-channel>single-channel. The channel combinations with the maximum Acc Best value of chb01 and chb10 on single-channel, two-channel and three-channel are respectively Channel 2, Channel 2,3 and Channel 1,3,5, Acc Best corresponding to 0.9645,0.9762595 and 0.973422, that is, two-channel>three-channel>single-channel (Figure 9-a). The averages of 23, 10 and 10 values of Average of chb01 and chb10 Acc Ave and Average of chb01 and chb10 Acc Best obtained are calculated (Figure 9-b). The results of the averages of Acc Ave and Acc best are both multi-channel>single-channel. In conclusion, the increase in the number of channels can tap potential for EEG signal recognition and

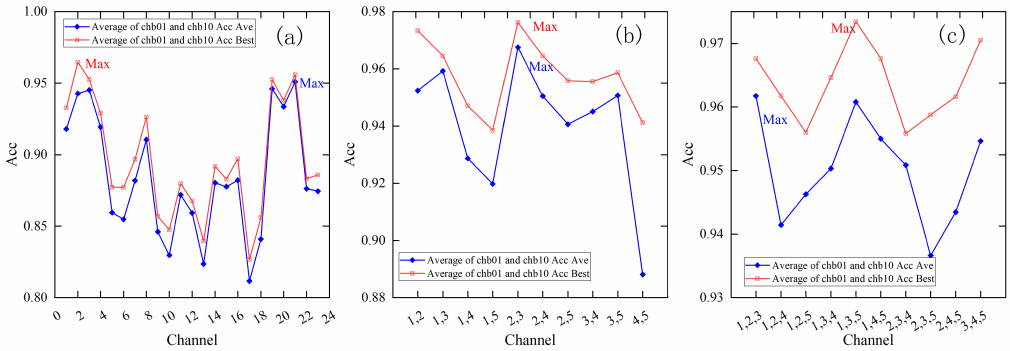

FIGURE 8. Comparison of multi-channel recognition results.

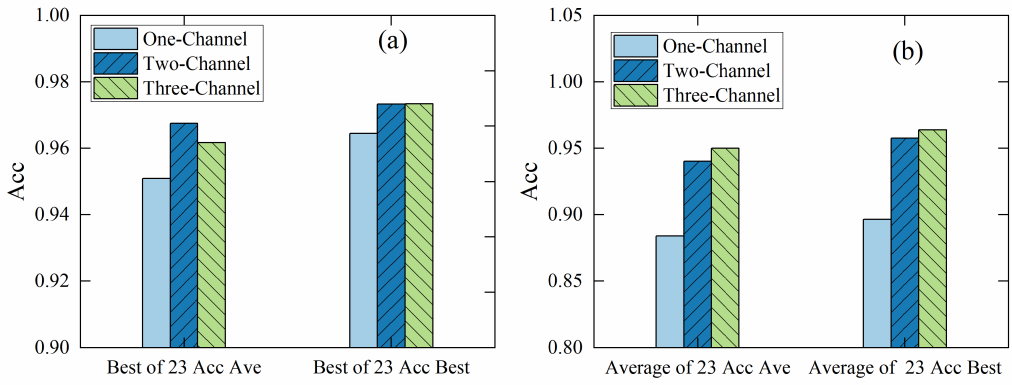

FIGURE 9. Comparison of multi-channel recognition results.

TABLE 9. Results based on bonn.

Database	Source of Comparison Method	Experimental Tool	Dimension of Network	Accuracy
Bonn	Turk O et al. [24]	MATLAB	1D network	1
Bonn	Liu J et al. [25]	Keras	1D network	0.996
Bonn	Ahmedt-Aristizabal D et al. [26]	Keras	2D network	0.9125
Bonn	Sharathappriyaa V et al. [27]	MATLAB	2D network	0.9867
Bonn	VarChanNet	pyTorch	1D network	0.975

TABLE 10. Results based on CHB-MIT.

Database	Comparison Method Source	Experimental Tool	Network Dimension	Accuracy
CHB-MIT	Ammar S et al. [17]	pyTorch	1D network	0.9485
CHB-MIT	Tian X B et al. [3]	pyTorch	1D network	0.9833
CHB-MIT	Yuan Y et al. [28]	pyTorch	2D network	0.9437
CHB-MIT	Ozdemir M A et al. [19]	pyTorch	2D network	0.9963
CHB-MIT	VarChanNet	pyTorch	1D network	0.9763

improve the accuracy of EEG signal recognition to a certain extent.

V. DISCUSSION

Most researches are carried out on a single EEG signal database. The comparison results of VarChanNet and comparative methods are shown in Table 9-10 and Figure 10. Table 9 compares VarChanNet with the method that carries out experiments based on Bonn database and Table 10 compares VarChanNet with that based on CHB-MIT database. Although the two groups of experiments are carried out based on the same EEG signal database, the EEG signal segmentation algorithms of different EEG signal recognition methods are different. As a result, the input data of these recognition methods are difficult to be consistent. The methods for EEG signal recognition that carry out experiments based on Bonn database are grouped and their precision of seizure recognition, such as VarScaleNet,

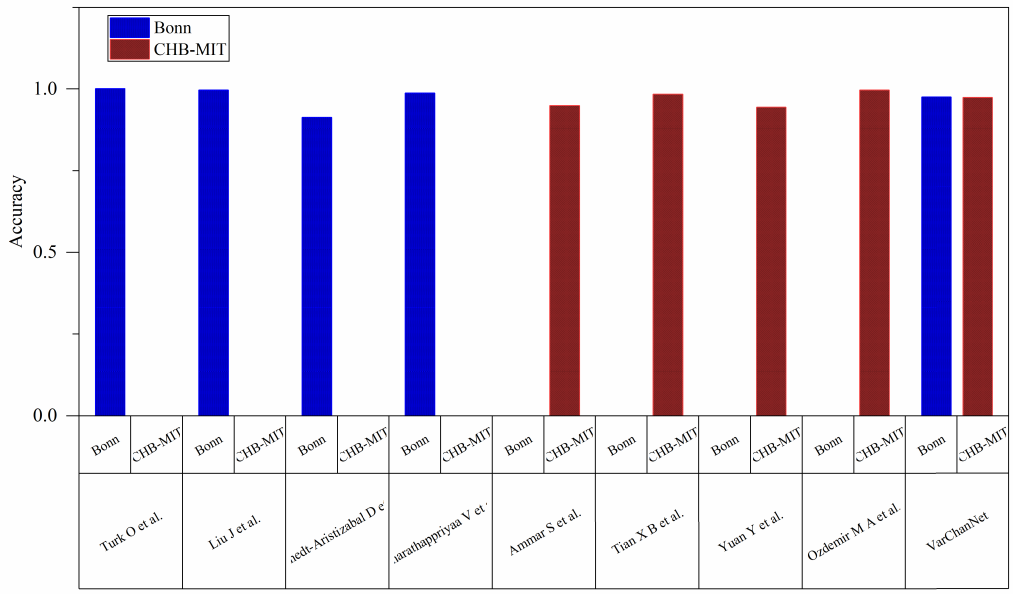

FIGURE 10. Results of comparison.

can reach 0.975, which is superior to the recognition results of the Ahmedt-Aristizabal D et al. group. The methods for seizure recognition that carry out experiments based on CHB-MIT database are grouped and VarScaleNet can achieve a precision of 0.9763, which is better than the Ammar S et al. and Yuan Y et al. groups. At present, most algorithms carry out experiments and tests on one database. Compared with existing studies, the VarScaleNet can realize seizure recognition on both Bonn database and CHB-MIT database on the premise of ensuring the accuracy of recognition result, which has a broader application prospect.

VI. CONCLUSION AND FUTURE WORK

In this study, a deep neural network is established based on dynamic routing algorithm and a recognition method for seizure, VarChanNet, is proposed based on this network. This method can change the structure of deep neural network according to the number of channels involved in recognition operation, obtain effective information from the channels and fuse the acquired effective information to realize EEG recognition of epileptic seizures. In this study, experiments are carried out on two different open epileptic EEG database to evaluate the performance of VarScaleNet. The important conclusions of the study are as follows:

1) The change of channel will affect the accuracy of the recognition result. On CHB-MIT database, Channel 21 can be selected on single- channel mode, Channel 2,3 can be selected on two-channel, and Channel 1,2,3 can be selected on three-channel.
2) The results of single-channel, two-channel and three-channel experiments show that the increase in the number of channels can tap potential for EEG signal recognition.
3) VarScaleNet conducted experiments on the Bonn and CHB-MIT databases and achieved impressive performance, indicating that the proposed method has generalization potential.

In future research, we will focus on exploring the fusion of multimodal data, aiming to extract recognition information contained in different modal data and achieve accurate recognition of epilepsy and other brain diseases.

REFERENCES

[1] N. Qi, Y. Piao, H. Zhang, Q. Wang, and Y. Wang, "Seizure prediction based on improved vision transformer model for EEG channel optimization," *Comput. Methods Biomechanics Biomed. Eng.*, vol. 2024, pp. 1–12, Mar. 2024.

[2] Y. Tian, C. Tan, Q. Wu, and Y. Zhou, "EEG epileptic seizure classification using hybrid time-frequency attention deep network," *Commun. Comput. Inf. Sci.*, vol. 1964, pp. 101–113, Nov. 2024.

[3] X. Tian, Z. Deng, W. Ying, K.-S. Choi, D. Wu, B. Qin, J. Wang, H. Shen, and S. Wang, "Deep multi-view feature learning for EEG-based epileptic seizure detection," *IEEE Trans. Neural Syst. Rehabil. Eng.*, vol. 27, no. 10, pp. 1962–1972, Oct. 2019.

[4] N. T. Anh-Dao, N. Linh-Trung, L. V. Nguyen, T. Tran-Duc, N. T. H. Anh, and B. Boashash, "A multistage system for automatic detection of epileptic spikes," *REV J. Electron. Commun.*, vol. 8, nos. 1–2, Jun. 2018.

[5] K. K. Dutta, P. Manohar, and K. Indira, "Time and frequency domain pre-processing for epileptic seizure classification of epileptic EEG signals," *J. Intell. Fuzzy Syst.*, vol. 45, no. 5, pp. 8217–8226, Nov. 2023.

[6] N. Ghassemi, A. Shoeibi, M. Rouhani, and H. Hosseini-Nejad, "Epileptic seizures detection in EEG signals using TQWT and ensemble learning," in *Proc. 9th Int. Conf. Comput. Knowl. Eng. (ICCKE)*, Oct. 2019, pp. 403–408.

[7] L. Vareka, "Comparison of convolutional and recurrent neural networks for the P300 detection," in *Proc. Biosignals*, 2021, pp. 186–191.

[8] G. Singer, A. Ratnovsky, and S. Naftali, "Classification of severity of trachea stenosis from EEG signals using ordinal decision-tree based algorithms and ensemble-based ordinal and non-ordinal algorithms," *Expert Syst. Appl.*, vol. 173, Jul. 2021, Art. no. 114707.

[9] Y. Zhang, Y. Zhang, J. Wang, and X. Zheng, "Comparison of classification methods on EEG signals based on wavelet packet decomposition," *Neural Comput. Appl.*, vol. 26, no. 5, pp. 1217–1225, Jul. 2015.

[10] J. Na, Z. Wang, S. Lv, and Z. Xu, "An extended K nearest neighbors-based classifier for epilepsy diagnosis," *IEEE Access*, vol. 9, pp. 73910–73923, 2021.
[11] S. K. Prabhakar, H. Rajaguru, and S.-W. Lee, "A framework for schizophrenia EEG signal classification with nature inspired optimization algorithms," *IEEE Access*, vol. 8, pp. 39875–39897, 2020.
[12] N. Memon, S. S. H. Zaidi, and M. Suleman, "The prognosis of epilepsy with naive Bayes classifier on FPGA using HDL coder," in *Proc. IEEE-EMBS Conf. Biomed. Eng. Sci. (IECBES)*, Mar. 2021, pp. 18–23.
[13] H. Zeng, C. Yang, G. Dai, F. Qin, J. Zhang, and W. Kong, "EEG classification of driver mental states by deep learning," *Cognit. Neurodynamics*, vol. 12, no. 6, pp. 597–606, Dec. 2018.
[14] A. Antoniades, L. Spyrou, D. Martin-Lopez, A. Valentin, G. Alarcon, S. Sanei, and C. Cheong Took, "Detection of interictal discharges with convolutional neural networks using discrete ordered multichannel intracranial EEG," *IEEE Trans. Neural Syst. Rehabil. Eng.*, vol. 25, no. 12, pp. 2285–2294, Dec. 2017.
[15] Y. Ganin, E. Ustinova, H. Ajakan, P. Germain, H. Larochelle, F. Laviolette, M. Marchand, and V. Lempitsky, "Domain-adversarial training of neural networks," *J. Mach. Learn. Res.*, vol. 17, no. 1, pp. 2030–2096, 2016.
[16] J. Thomas, L. Comoretto, J. Jin, J. Dauwels, S. S. Cash, and M. B. Westover, "EEG CLassification via convolutional neural network-based interictal epileptiform event detection," in *Proc. 40th Annu. Int. Conf. IEEE Eng. Med. Biol. Soc. (EMBC)*, Jul. 2018, pp. 3148–3151.
[17] S. Ammar and M. Senouci, "Seizure detection with single-channel EEG using extreme learning machine," in *Proc. 17th Int. Conf. Sci. Techn. Autom. Control Comput. Eng. (STA)*, Dec. 2016, pp. 776–779.
[18] L. Sui et al., "Localization of epileptic foci by using convolutional neural network based on iEEG," in *Artificial Intelligence Applications and Innovations: 15th IFIP WG 12.5 International Conference, AIAI 2019, Hersonissos, Crete, Greece, May 24–26, 2019, Proceedings 15*. Springer, 2019, pp. 331–339.
[19] M. A. Ozdemir, O. K. Cura, and A. Akan, "Epileptic EEG classification by using time-frequency images for deep learning," *Int. J. Neural Syst.*, vol. 31, no. 8, Aug. 2021, Art. no. 2150026.
[20] A. Shoeibi, M. Khodatars, N. Ghassemi, M. Jafari, P. Moridian, R. Alizadehsani, M. Panahiazar, F. Khozeimeh, A. Zare, H. Hosseini-Nejad, A. Khosravi, A. F. Atiya, D. Aminshahidi, S. Hussain, and M. Rouhani, "Epileptic seizures detection using deep learning techniques: A review," *Int. J. Environ. Res. Public Health*, vol. 18, no. 11, p. 5780, 2021.
[21] S. Alhagry, A. Aly, and R. A. El-Khoribi, "Emotion recognition based on EEG using LSTM recurrent neural network," *Int. J. Adv. Comput. Sci. Appl.*, vol. 8, no. 10, pp. 355–358, 2017.
[22] K. M. Tsiouris, V. C. Pezoulas, M. Zervakis, S. Konitsiotis, D. D. Koutsouris, and D. I. Fotiadis, "A long short-term memory deep learning network for the prediction of epileptic seizures using EEG signals," *Comput. Biol. Med.*, vol. 99, pp. 24–37, Aug. 2018.
[23] J. Turner, A. Page, T. Mohsenin, and T. Oates, "Deep belief networks used on high resolution multichannel electroencephalography data for seizure detection," in *Proc. AAAI spring Symp. Ser.*, 2014, pp. 75–81.
[24] Ö. Türk and M. S. Özerdem, "Epilepsy detection by using scalogram based convolutional neural network from EEG signals," *Brain Sci.*, vol. 9, no. 5, p. 115, May 2019.
[25] J. Liu and B. Woodson, "Deep learning classification for epilepsy detection using a single channel electroencephalography (EEG)," in *Proc. 3rd Int. Conf. Deep Learn. Technol.*, Jul. 2019, pp. 23–26.
[26] D. Ahmedt-Aristizabal, C. Fookes, K. Nguyen, and S. Sridharan, "Deep classification of epileptic signals," in *Proc. 40th Annu. Int. Conf. IEEE Eng. Med. Biol. Soc. (EMBC)*, Jul. 2018, pp. 332–335.
[27] V. Sharathappriyaa, S. Gautham, and R. Lavanya, "Auto-encoder based automated epilepsy diagnosis," in *Proc. Int. Conf. Adv. Comput., Commun. Informat. (ICACCI)*, Sep. 2018, pp. 976–982.
[28] Y. Yuan, G. Xun, K. Jia, and A. Zhang, "A multi-view deep learning framework for EEG seizure detection," *IEEE J. Biomed. Health Informat.*, vol. 23, no. 1, pp. 83–94, Jan. 2019.

ZHIWEN XIONG received the Ph.D. degree from the School of Computer and Information Science, Hohai University, Nanjing, China. He is currently engaged in scientific research with Yiwu Industrial and Commercial College. His research interests include biomedical signal processing and wireless sensor networks.

YANG LIU received the master's degree from the School of Computer Science, Hangzhou Dianzi University. He is a full-time Computer Teacher with the School of Artificial Intelligence, Chongqing College of Science and Creation. His main research interests include deep learning, EEG signal classification, and cognitive computing.

PENG JIANG received the Ph.D. degree in management science and engineering from Jiangxi University of Finance and Economics, China. He is currently an Associate Professor with Yiwu Industrial and Commercial College, China. His research interests include network security and privacy protection, user continuance behavior in mobile social network and emergency decision support systems. He received the William F. Meggers Award and the Adolph Lomb Medal (OSA).